Regional and seasonal radiative forcing by perturbations to aerosol and ozone precursor emissions

Bellouin et al.

Supplementary Figures

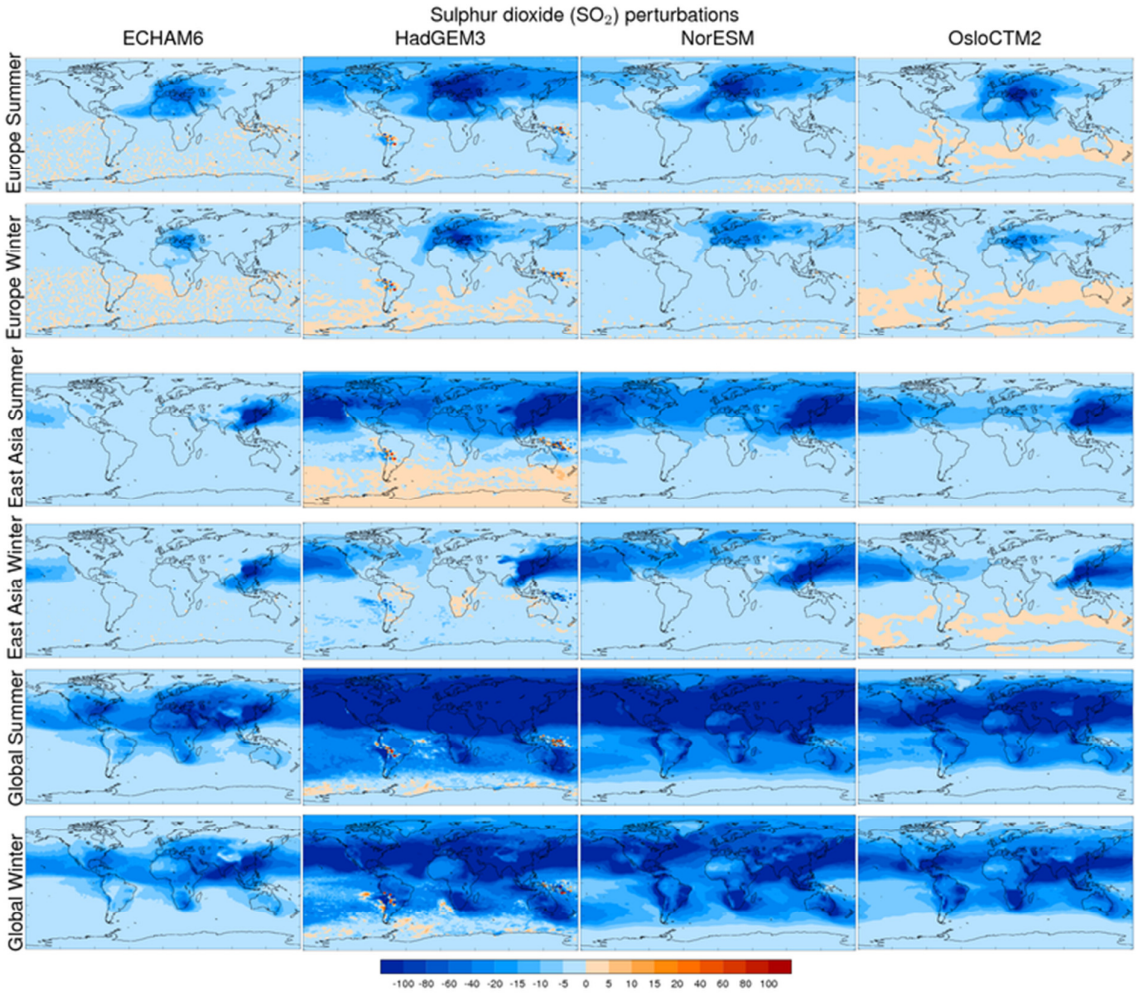

Figure S1. Annually-averaged radiative forcing of aerosol-radiation and aerosol-cloud interactions, in mW m^{-2}, exerted by regional and seasonal perturbation (rows) of sulphur dioxide emissions in four models (columns). Note that the colour scale is not linear.

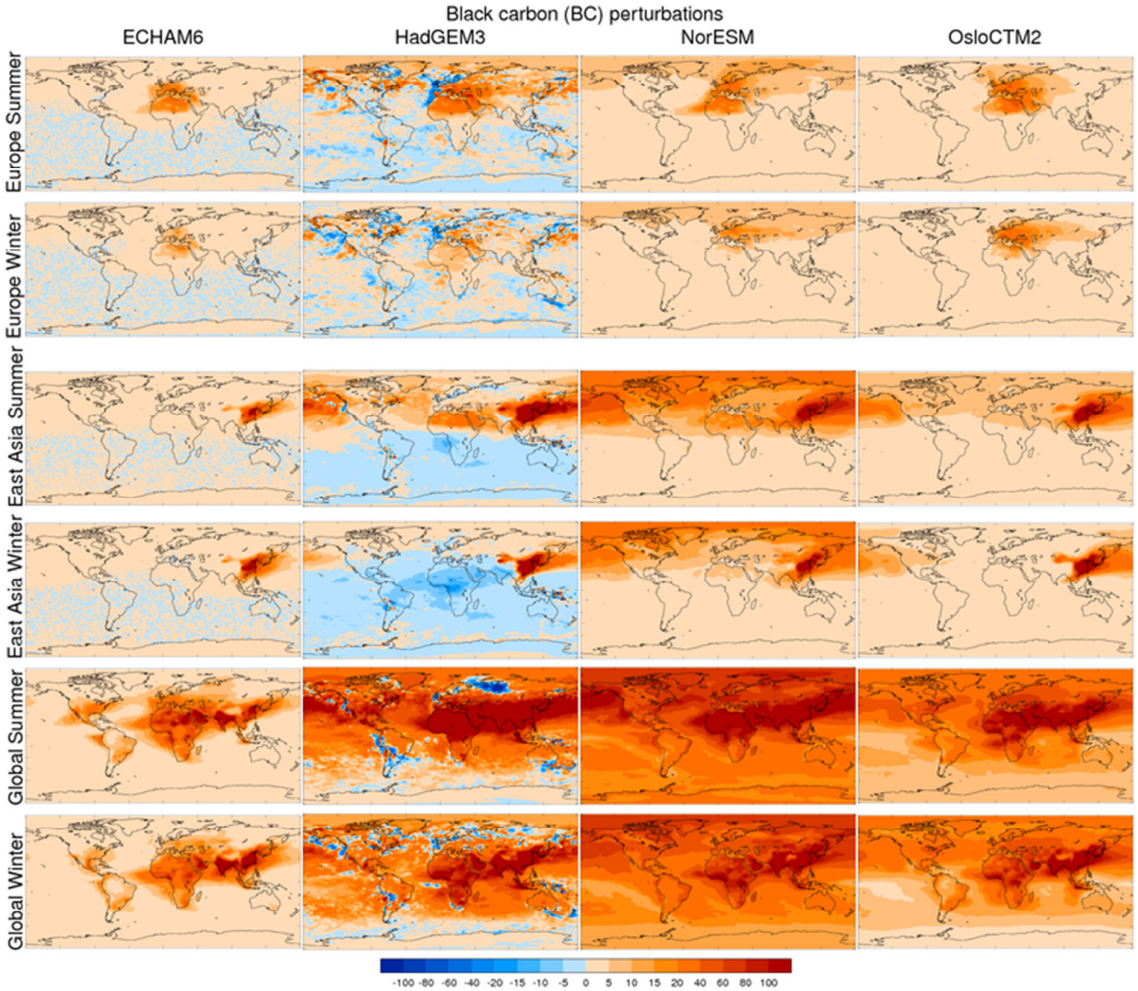

Figure S2. Annually-averaged radiative forcing of aerosol-radiation and aerosol-cloud interactions, in mW m^{-2}, exerted by regional and seasonal perturbation (rows) of primary black carbon emissions in four models (columns). Note that the colour scale is not linear.

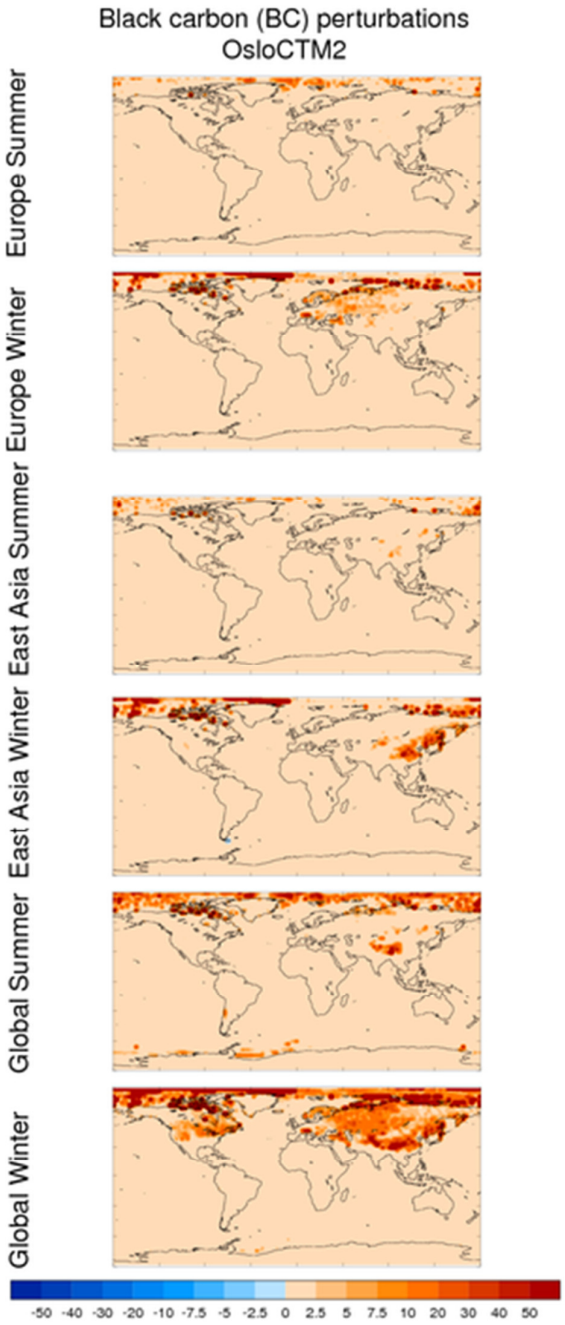

Figure S3. Annually-averaged radiative forcing of black carbon deposition on snow, in mW m^{-2}, exerted by regional and seasonal perturbation (rows) of primary black carbon emissions in the OsloCTM2 model. Note that the colour scale is not linear, and has been magnified by a factor 2 compared to most other Figures in this supplement.

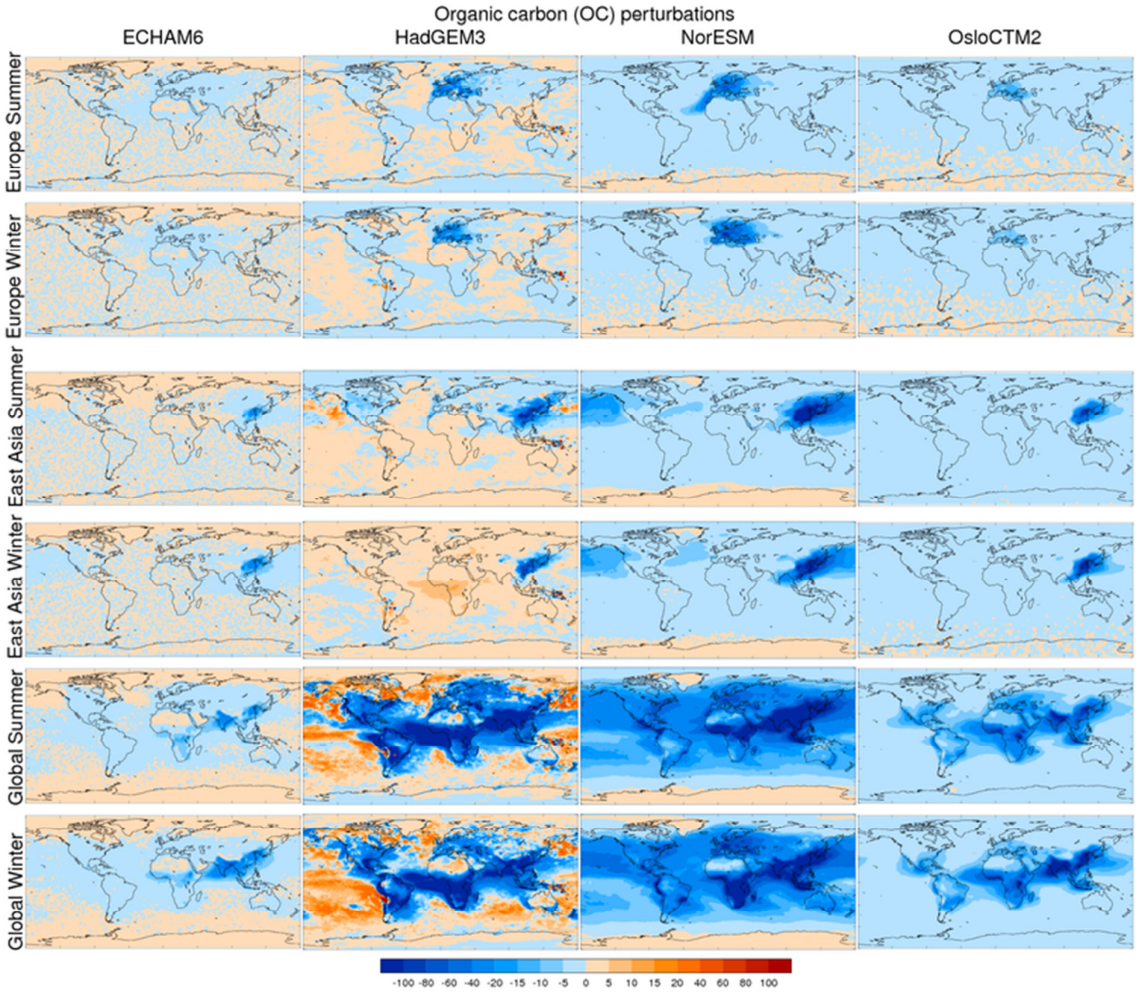

Figure S4. Annually-averaged radiative forcing of aerosol-radiation and aerosol-cloud interactions, in mW m^{-2}, exerted by regional and seasonal perturbation (rows) of primary emissions of organic carbon aerosols in four models (columns). Note that the colour scale is not linear.

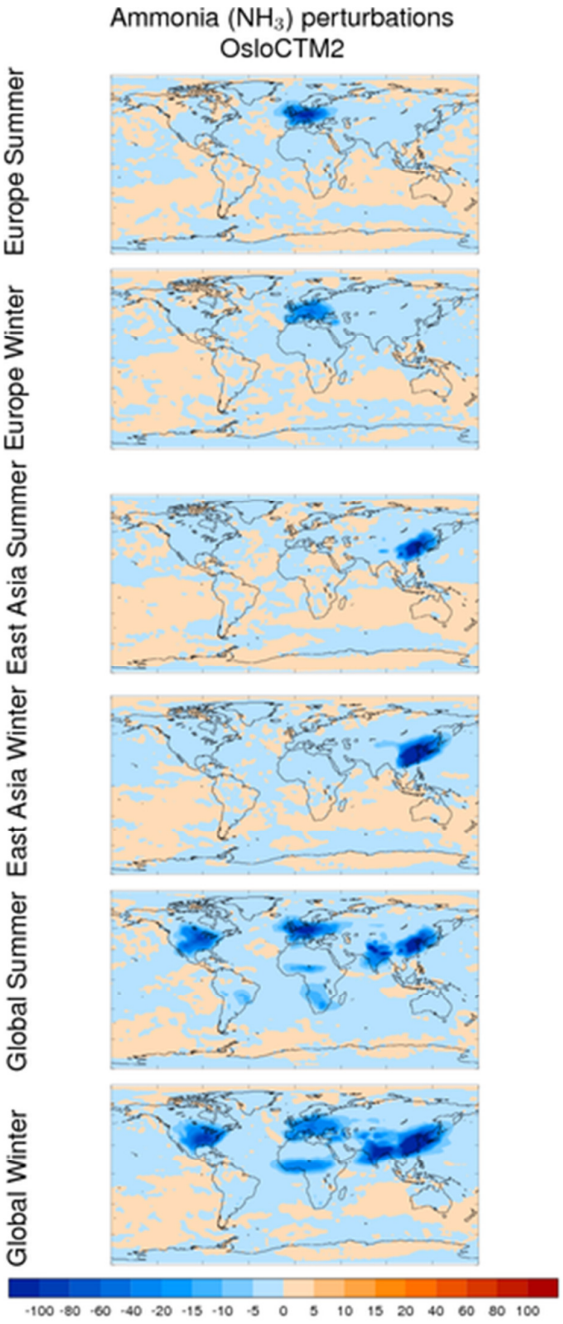

Figure S5. Annually-averaged radiative forcing of aerosol-radiation and aerosol-cloud interactions, in mW m^{-2}, exerted by regional and seasonal perturbation of ammonia emissions the OsloCTM2 model. Note that the colour scale is not linear.

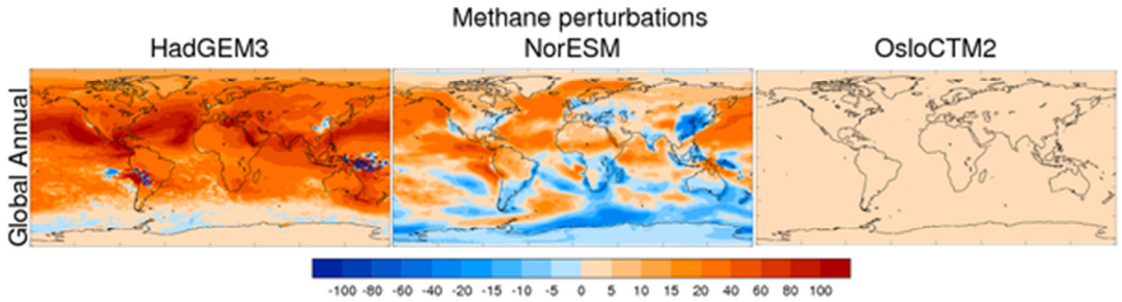

Figure S6. Annually-averaged radiative forcing of aerosol-radiation and aerosol-cloud interactions, in mW m^{-2}, exerted by global and annual perturbation of methane mass mixing ratios in three models (columns). Distributions for OsloCTM2 are not available (see section 3.5), so its distribution is left empty for the sake of consistency with other Figures. Note that the colour scale is not linear.

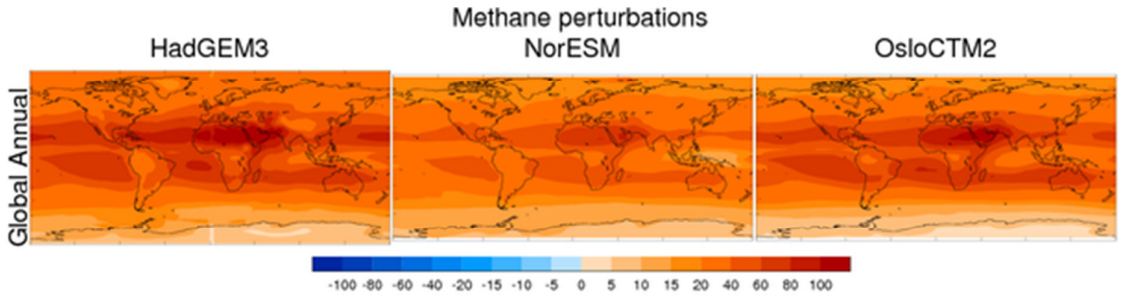

Figure S7. Annually-averaged radiative forcing by direct changes in ozone, in mW m^{-2}, exerted by global and annual perturbation of methane mass mixing ratios in three models (columns). Note that the colour scale is not linear.

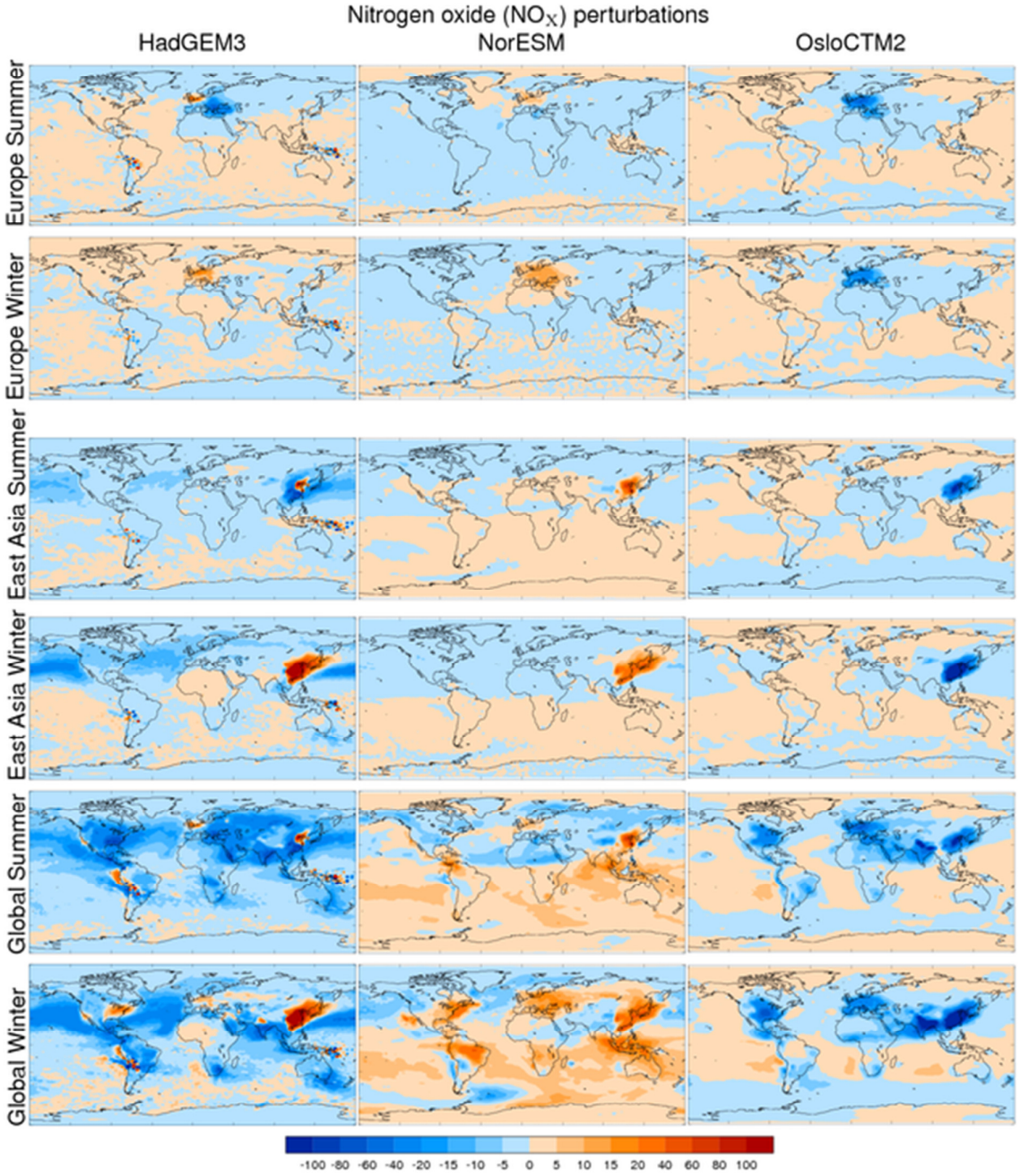

Figure S8. Annually-averaged radiative forcing of aerosol-radiation and aerosol-cloud interactions, in mW m^{-2}, exerted by regional and seasonal perturbation (rows) of emissions of nitrogen oxides in three models (columns). Note that the colour scale is not linear.

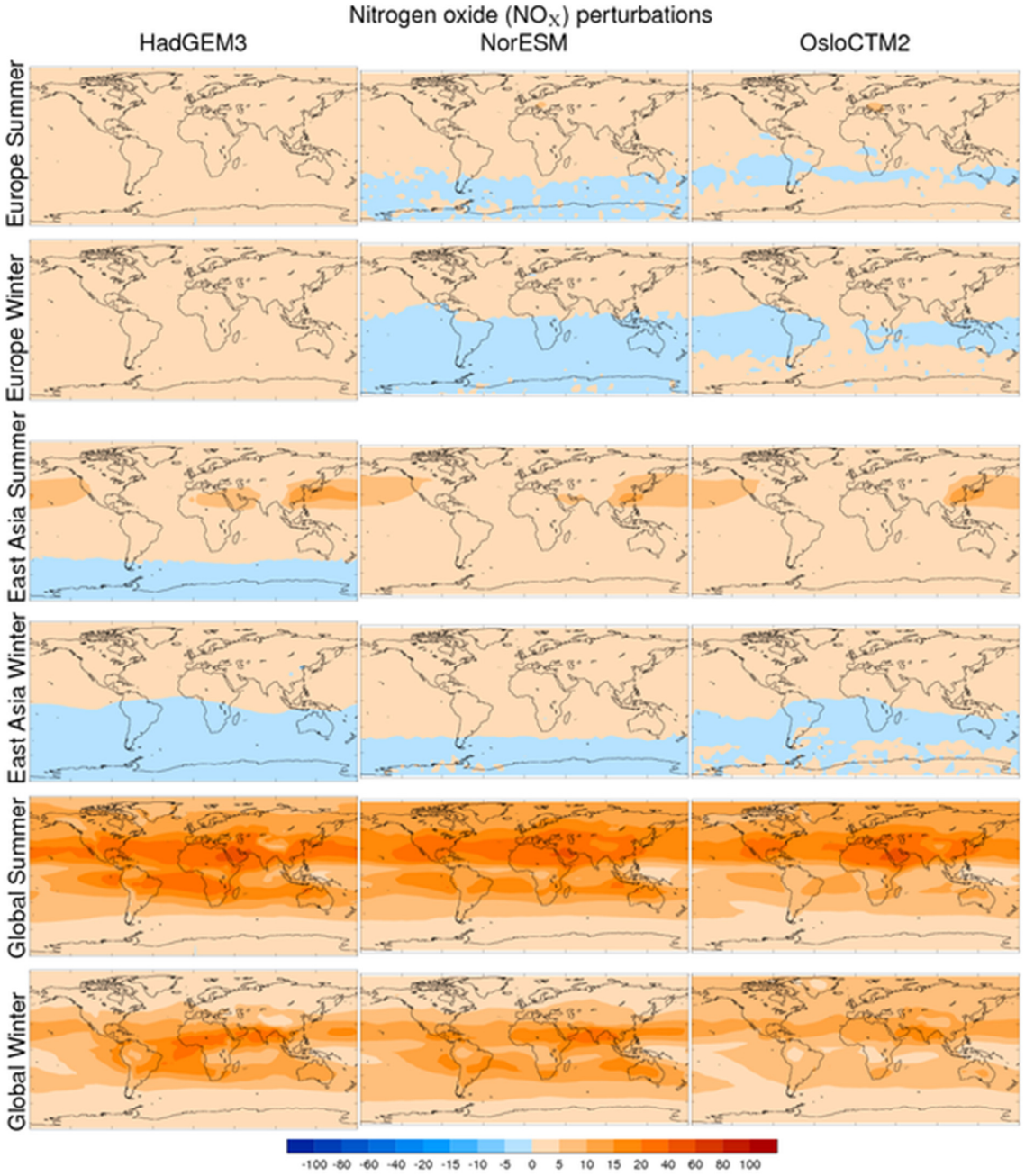

Figure S9. Annually-averaged radiative forcing by direct changes in ozone, in mW m^{-2}, exerted by regional and seasonal perturbation (rows) of emissions of nitrogen oxides in three models (columns). Note that the colour scale is not linear.

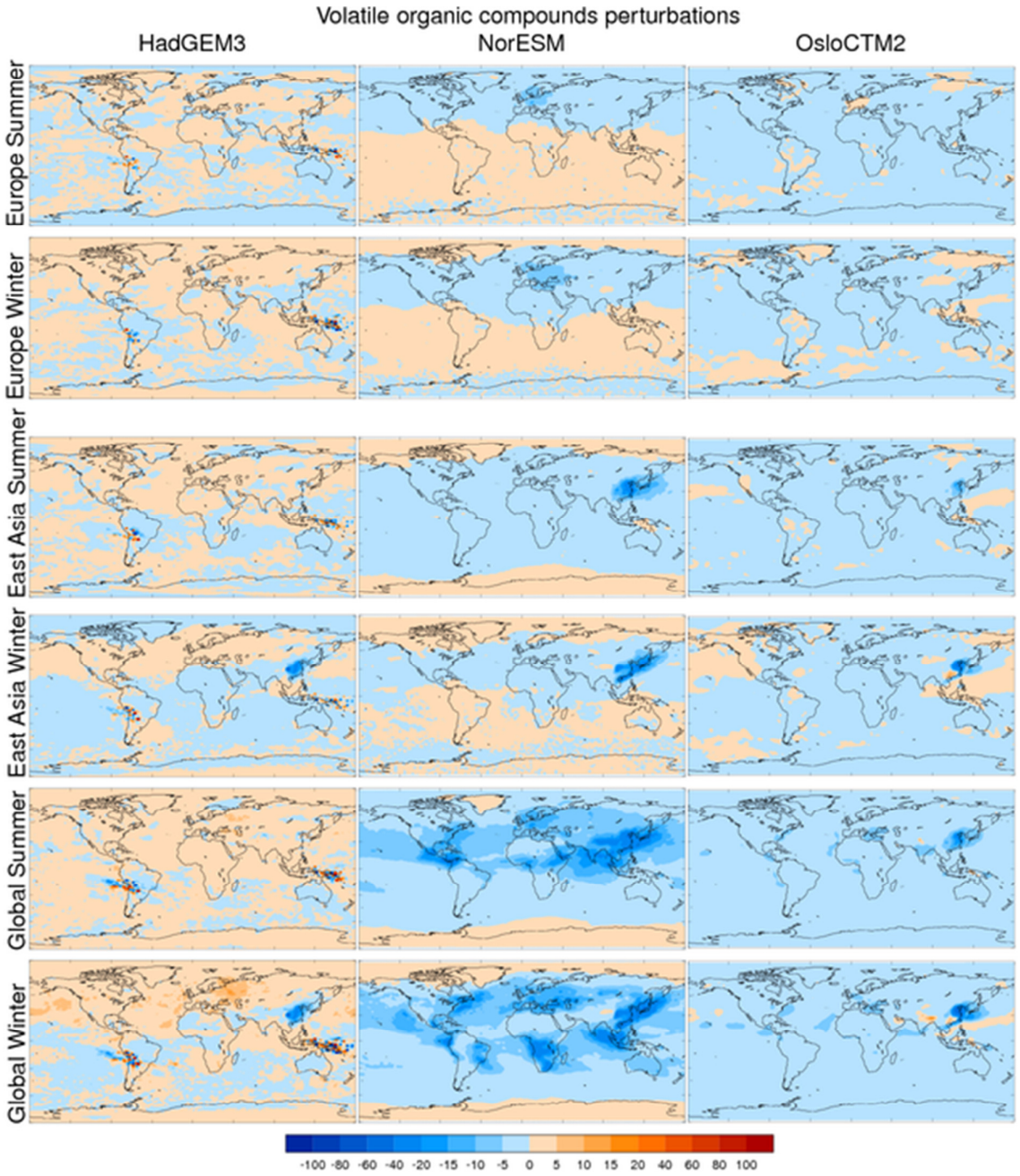

Figure S10. Annually-averaged radiative forcing of aerosol-radiation and aerosol-cloud interactions, in mW m^{-2}, exerted by regional and seasonal perturbation (rows) of emissions of non-methane volatile organic compounds in three models (columns). Note that the colour scale is not linear.

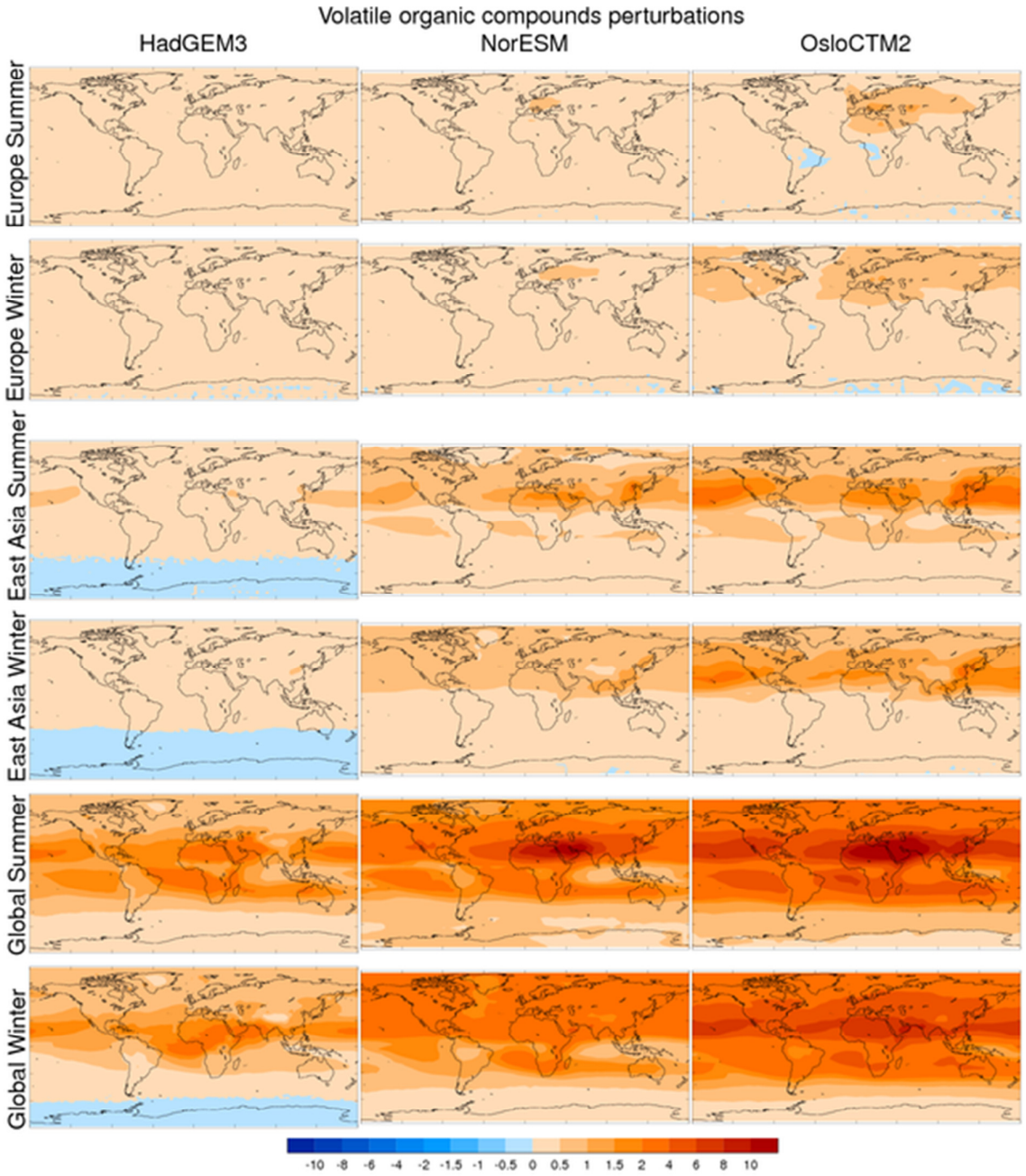

Figure S11. Annually-averaged radiative forcing by direct changes in ozone, in mW m^{-2}, exerted by regional and seasonal perturbation (rows) of emissions of non-methane volatile organic compounds in three models (columns). Note that the colour scale is not linear, and has been magnified by a factor 10 compared to most other Figures in this supplement.

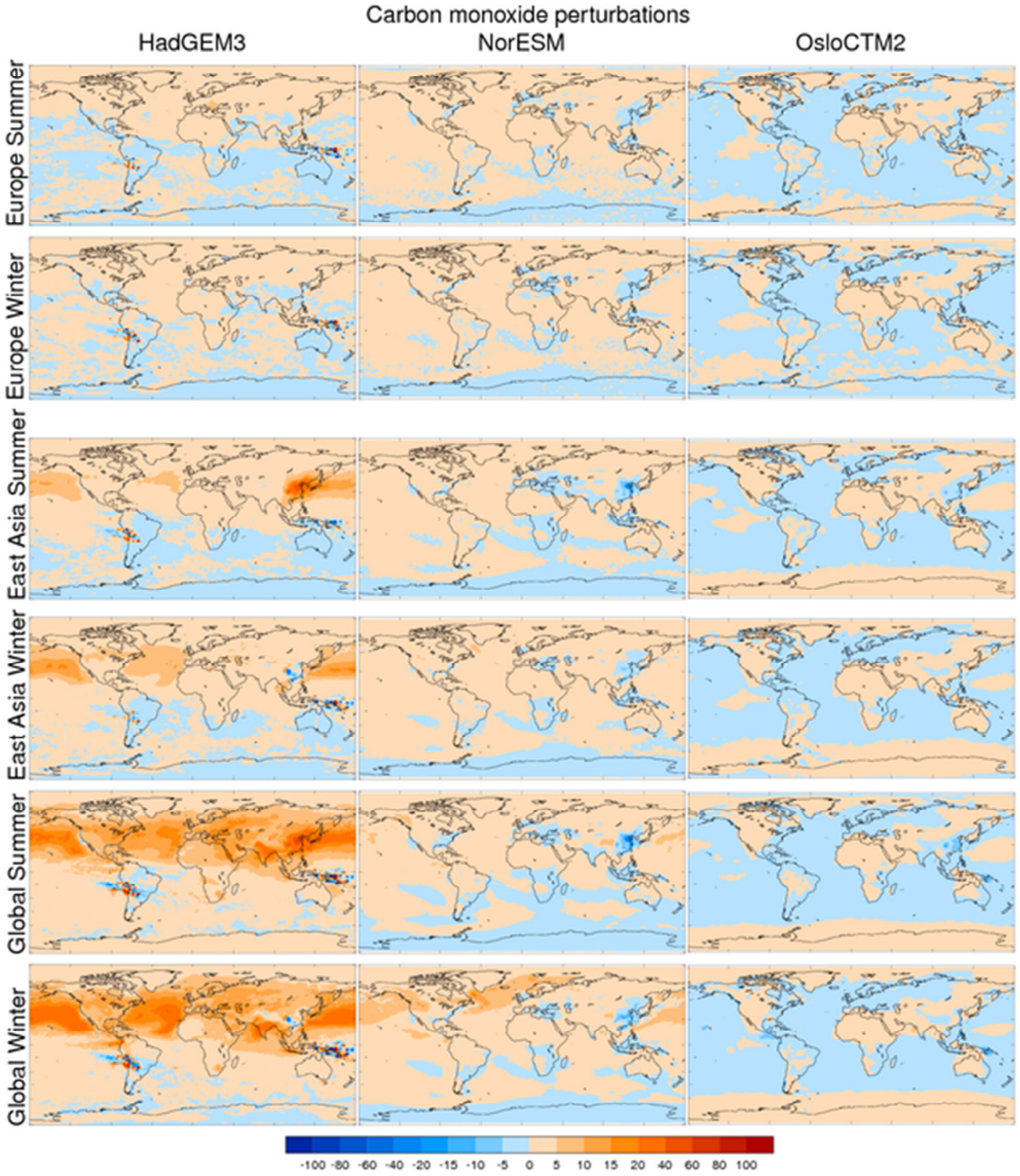

Figure S12. Annually-averaged radiative forcing of aerosol-radiation and aerosol-cloud interactions, in mW m^{-2}, exerted by regional and seasonal perturbation (rows) of emissions of carbon monoxide in three models (columns). Note that the colour scale is not linear.

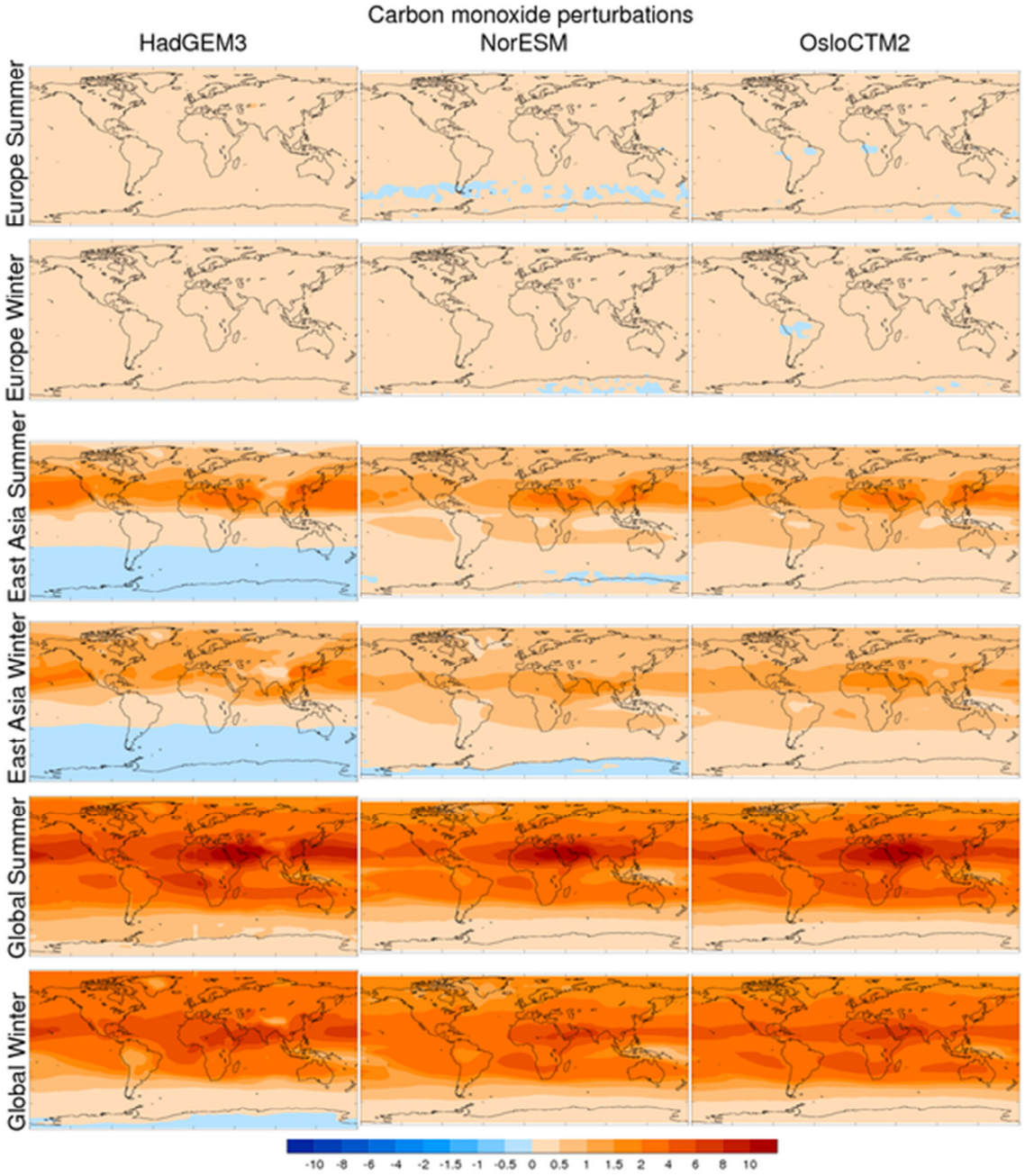

Figure S13. Annually-averaged radiative forcing by direct changes in ozone, in mW m^{-2}, exerted by regional and seasonal perturbation (rows) of emissions of carbon monoxide in three models (columns). Note that the colour scale is not linear, and has been magnified by a factor 10 compared to most other Figures in this supplement.

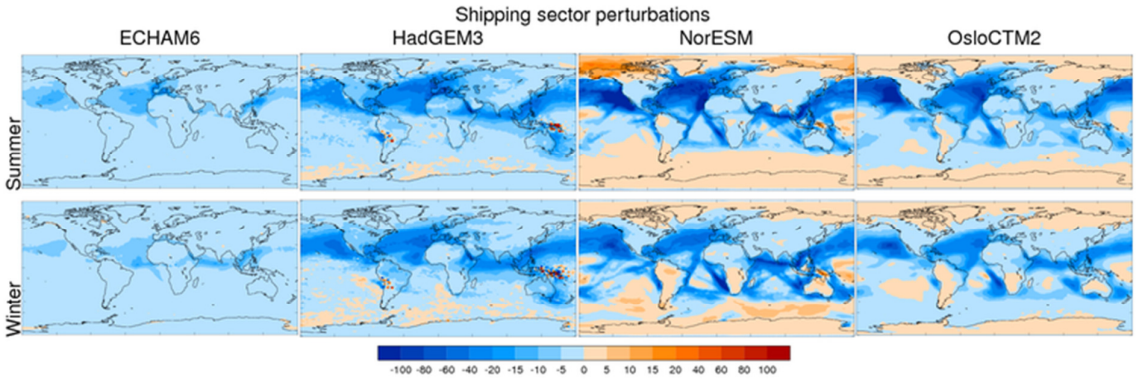

Figure S14. Annually-averaged radiative forcing of aerosol-radiation and aerosol-cloud interactions, in mW m^{-2}, exerted by seasonal perturbation (rows) of all species emitted by the shipping sector in four models (columns). Note that the colour scale is not linear.

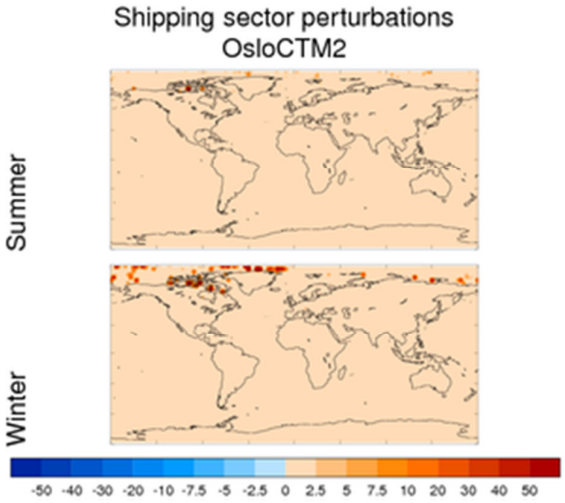

Figure S15. Annually-averaged radiative forcing of black carbon deposition on snow, in mW m^{-2}, exerted by seasonal perturbation (rows) of primary black carbon emissions from the shipping sector in the OsloCTM2 model. Note that the colour scale is not linear, and has been magnified by a factor 2 compared to most other Figures in this supplement.

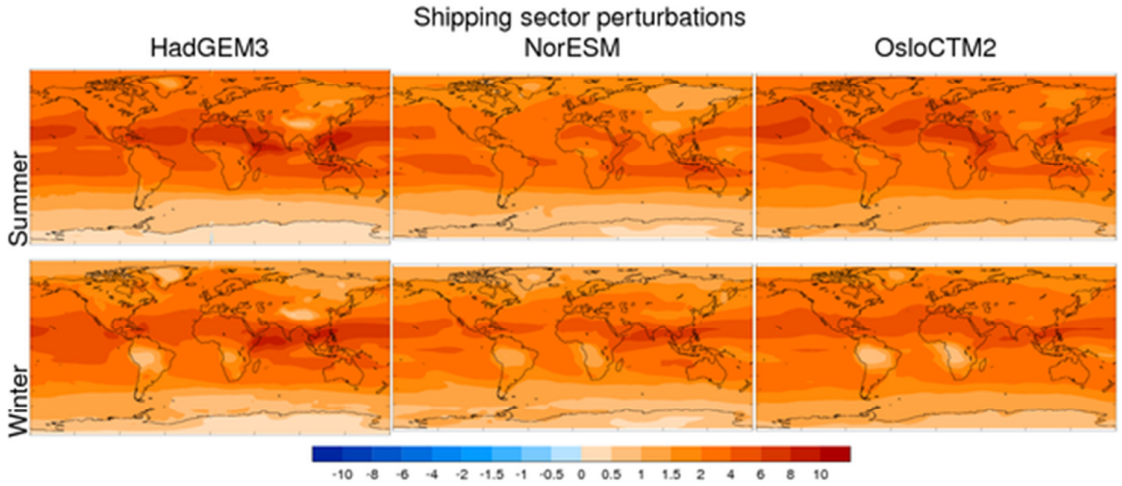

Figure S16. Annually-averaged radiative forcing by direct changes in ozone, in mW m^{-2}, exerted by regional and seasonal perturbation (rows) of all species emitted by the shipping sector in three models (columns). Note that the colour scale is not linear, and has been magnified by a factor 10 compared to most other Figures in this supplement.

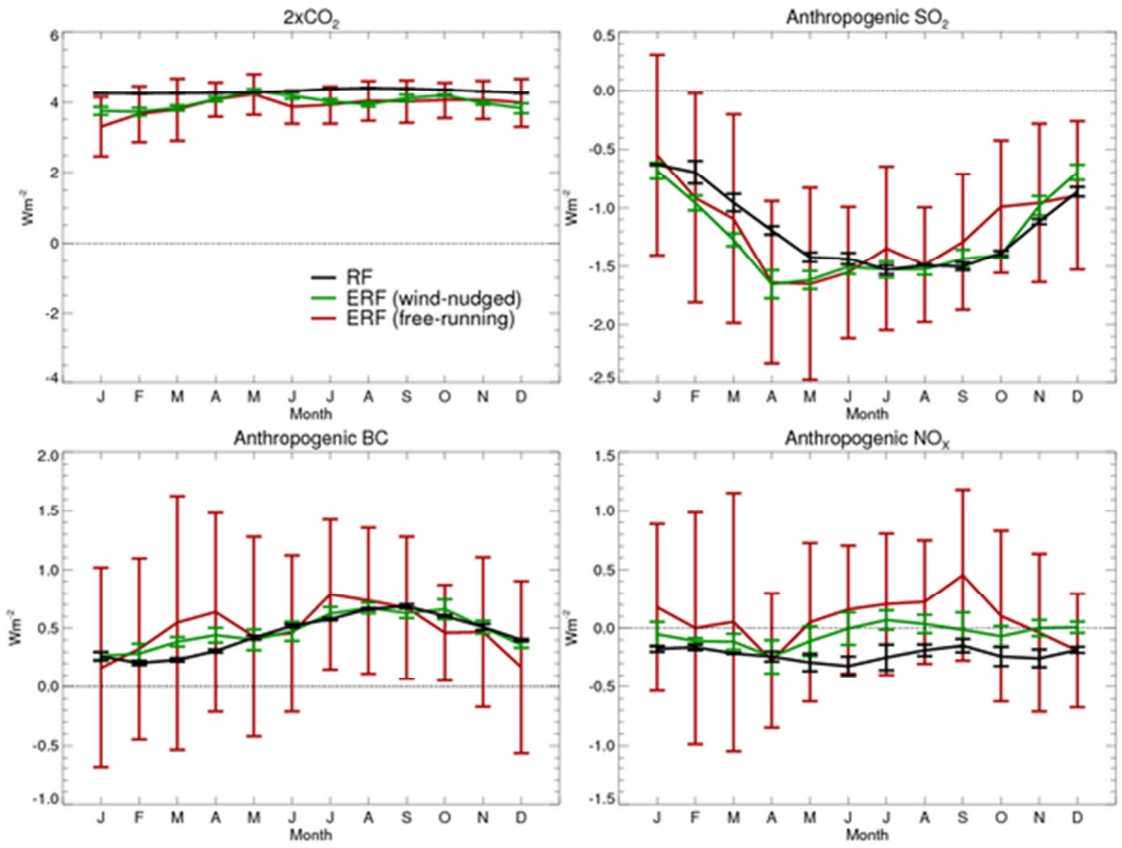

Figure S17. Multi-annual monthly and global mean radiative forcing (black, from 3-year simulations), effective radiative forcing with nudged wind speeds (green, from 5-year simulations), and effective radiative forcing without nudging (brown, from 20-year simulations), for (clockwise from top left) a doubling of carbon dioxide concentrations; industrial-era increases in sulphur dioxide emissions; industrial-era increases in nitrogen oxide emissions; and industrial-era increases in black carbon emissions. Whiskers show the inter-annual standard deviations for each month. All simulations by the HadGEM3 model.

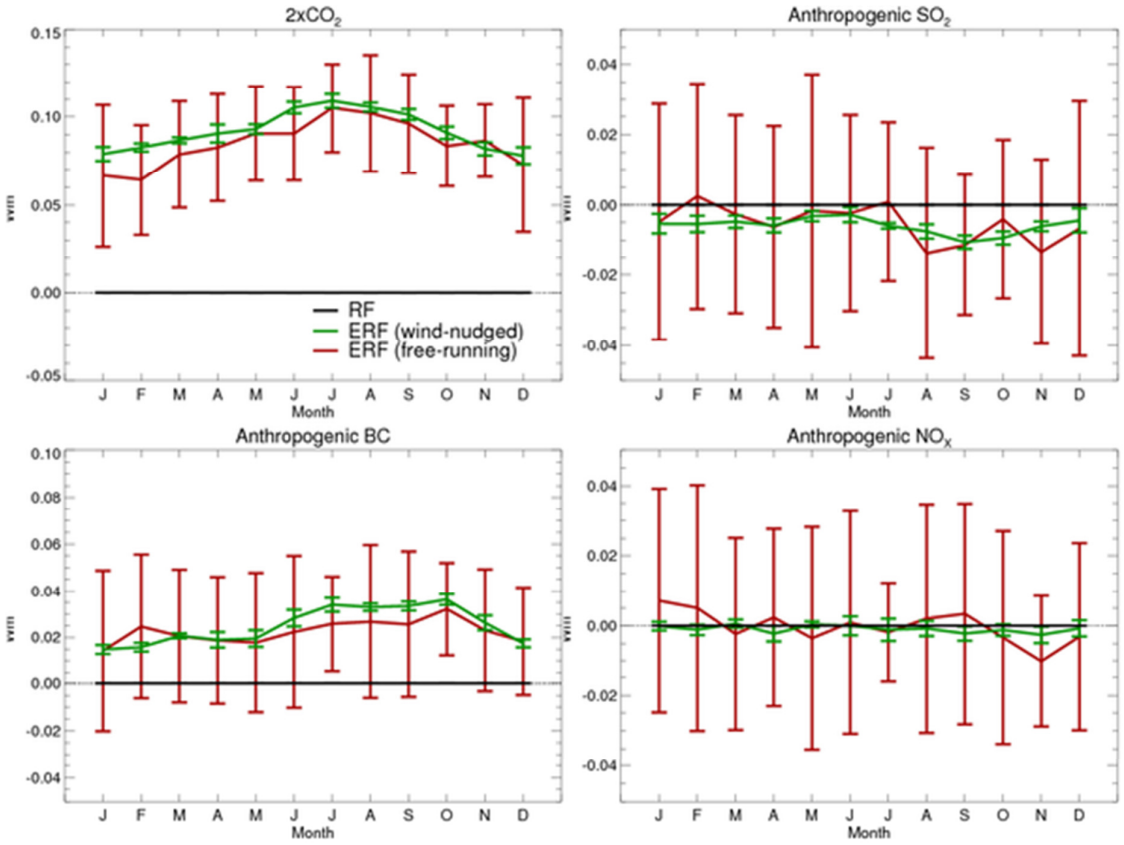

Figure S18. As Figure S17, but for globally-averaged changes in precipitation rate.